Spaceflight Effects and Molecular Responses in the Mouse Eye: Preliminary Observations After Shuttle Mission STS-133

Susana B. Zanello[1], Corey A. Theriot[2], Claudia Maria Prospero Ponce[3] , and Patricia Chevez-Barrios[3,4]

[1] *Division of Space Life Sciences, Universities Space Research Association, Houston, TX;* [2] *Wyle Science, Technology and Engineering, Houston, TX, Department of Preventive Medicine and Community Health, University of Texas Medical Branch, Galveston, TX;* [3] *Pathology and Laboratory Medicine and Ophthalmology, Weill Medical College of Cornell University, The Methodist Hospital, Houston, TX;* [4] *Department of Pathology and Genomic Medicine, The Methodist Hospital, Houston, TX*

ABSTRACT

Spaceflight exploration presents environmental stressors including microgravity-induced cephalad fluid shift and radiation exposure. Ocular changes leading to visual impairment in astronauts are of occupational health relevance. The effect of this complex environment on ocular morphology and function is poorly understood. Female 10-12 week-old BALB/cJ mice were assigned to a flight (FLT) group flown on shuttle mission STS-133, Animal Enclosure Module ground control group (AEM), or vivarium-housed (VIV) ground controls. Eyes were collected at 1, 5, and 7 days after landing and were fixed for histological sectioning. The contralateral eye was used for gene expression profiling by RT-qPCR. Sections were visualized by hematoxylin/eosin stain and processed for 8-hydroxy-2'-deoxyguanosine (8-OHdG), caspase-3, and glial fibrillary acidic protein (GFAP) and β-amyloid double-staining. 8-OHdG and caspase-3 immunoreactivity was increased in the retina in FLT samples at return from flight (R+1) compared to ground controls, and decreased at day 7 (R+7). β-amyloid was seen in the nerve fibers at the post-laminar region of the optic nerve in the flight samples (R+7). Expression of oxidative and cellular stress response genes was upregulated in the retina of FLT samples upon landing, followed by lower levels by R+7. These results suggest that reversible molecular damage occurs in the retina of mice exposed to spaceflight and that protective cellular pathways are induced in the retina and optic nerve in response to these changes.

INTRODUCTION

The space environment creates challenges for extended human spaceflight and presents a unique combination of stressors: microgravity, high-energy-particle radiation, nutritional deficiencies, hypobaric hypoxia, intermittent hyperoxia, and psychological stress. Lack of gravity implies reduced physical loading, fluid shift, and incompletely understood cellular responses that are reflected by a number of detrimental changes, such as muscle atrophy and loss of bone mass, immunosuppression, and overall gene expression changes (Pietsch et al., 2011; Sundaresan and Pellis, 2009). Ground models of simulated

microgravity, namely hindlimb suspension (HS) and bed rest, induce a fluid shift and concomitant vascular pressure and flow alterations (Hargens and Watenpaugh, 1996; Wilkerson *et al*., 2002), affecting not only cardiovascular physiology but also inducing genome-wide gene expression changes in the central nervous system (Frigeri et al., 2008).

Ocular changes have been reported related to exposure to the space environment. In humans, the direct effect of radiation in the lens results in cataract formation (Cucinotta *et al*., 2001), which manifests with a higher incidence and earlier onset in the astronaut population. Light flashes in the eye are an occurrence that has been observed by astronauts since the Apollo program (Sannita *et al*., 2006) -- a phenomenon not completely understood.

Most importantly, recent medical data from astronaut cohorts have reported the development of optic disc edema, choroidal folds, posterior globe flattening, and a resulting hyperopic shift (Kramer *et al*., 2012; Mader *et al.*, 2011) in a fraction of the astronaut population upon return from missions longer than 30 days (NASA, 2010). No clear etiology has been established for these cases, but it is hypothesized that microgravity, the ensuing cephalad fluid shift, and venous congestion may play a role. The perturbations observed in some individuals of the astronaut cohort resemble those found in papilledema associated with idiopathic intracranial hypertension (IIH) also known as pseudotumor cerebri (Friedman, 2007; Kramer *et al*., 2012; Mader *et al*., 2011). Because the etiology is still a matter of speculation, investigating whether exposure to microgravity represents a source of stress for the eye is an issue of critical occupational health importance. To this aim, this project examines the effects of spaceflight on the rodent eye and the responses that occur when challenged with exposure to microgravity in combination with other stressors during spaceflight.

Previous spaceflight studies performed on rodents found evidence of retinal degeneration in neonatal rats aboard shuttle mission STS-72 (Tombran-Tink and Barnstable, 2006), and of cell swelling and disruption in rats aboard two experiments on Russian Cosmos satellites (Philpott et al., 1980; Philpott et al., 1978).

However, these studies were limited to structural histopathologic observations of the eye. In the present work, we expand the immunohistopathologic analysis to investigate the effects of spaceflight and the elicited responses observed in the eyes of mice aboard shuttle mission STS-133, focusing, for the first time, on molecular and cellular processes subjacent to the histopathologic changes.

MATERIALS AND METHODS

Animals

This work consisted of a tissue sharing-derived project that used specimens collected from a parent animal experiment aboard shuttle mission STS-133. The original experiment included animals infected with respiratory syncytial virus immediately after return to Earth (study led by independent investigator Dr. Roberto Garofalo, from the University of Texas Medical Branch in Galveston). However, the work discussed in this article only included the non-infected control animals. Animal procedures were approved by the NASA Ames Research Center and Kennedy Space Center institutional animal care and use committees. The STS-133 mission occurred from February 24 to March 9, 2011, for a total duration of 12 days and 19 hours. Female 10 to 12 week-old BALB/cJ mice were assigned to one of three experimental groups: Flight (FLT), Animal Enclosure Module (AEM) ground controls, and vivarium-housed (VIV) ground controls. The flight animals (FLT) were housed in AEMs identical to the ground controls. The AEM is a self-contained habitat that provides ventilation, waste management, food, water, and controlled lighting (Naidu *et al*., 1995). It has previously been used in experiments studying rodent biology during spaceflight. The AEM flight unit is located in the middeck locker of the shuttle and its temperature is set at 3° to 8°C above the environmental middeck temperature. Lighting of 14 lux is set to a 12 hour day/12 hour night cycle. AEM ground controls were maintained in identical conditions at the Space Life Sciences Laboratory, Kennedy Space Center. Vivarium ground controls were housed in standard vivarium cages and conditions, on a 12-hour day/12-hour night light cycle at 200 to 215 lux. In view of the housing and lighting conditions

of the vivarium, the proper ground controls that allow measuring the effects attributed to spaceflight are the AEM-housed ground controls.

After sacrifice, one eye of each mouse from the three groups (FLT, AEM, and VIV) was collected at 1, 5, and 7 days after landing, and was fixed for histological examination. The contralateral eye was stored in RNALater and used for gene expression profiling by RT-qPCR.

Materials

The histological 4% paraformaldehyde-based fixative was obtained from Excalibur Pathology, Inc., Oklahoma City, OK. Goat polyclonal antibody to 8-hydroxy-2'-deoxyguanosine (8OHdG) (ab10802) and rabbit polyclonal antibody to activated caspase-3 (ab52181) were purchased from Abcam Inc., Cambridge, MA. Mouse monoclonal antibody to β-amyloid 1-16 was obtained from Millipore (Temecula, CA) and rabbit polyclonal antibody against glial fibrillary acidic protein (GFAP) was purchased from Dako, Carpinteria, CA. Paraffin embedding and histologic sectioning were contracted from Excalibur Pathology. qRT-PCR reagents were purchased from Qiagen Inc., Valencia, CA and BioRad, Hercules, CA. Tissue samples were assigned a different number for immunohistochemistry evaluation and gene profiling to perform a masked analysis.

Histology and Immunohistochemistry

Fixed eyes were paraffin embedded, sectioned at 5 μm thickness, and stained with standard hematoxylin-eosin (H&E) for histologic examination. Four immunohistologic stains were performed: 8OHdG to detect oxidative-related DNA damage, activated caspase-3 to study apoptosis, and double stain using β-amyloid as a marker of neuronal and axonal injury and GFAP as an indicator of glial activation. All immunostains had negative (omitting primary antibody) and positive (using known tissue that reacts with the antibody of interest) controls. For 8OHdG and caspase-3 staining, sections were equilibrated in water after deparaffinization and treated sequentially in 3% hydrogen peroxide, 1% acetic acid, and 2.5% serum (Vector Labs, Burlingame, CA) before incubating with the diluted primary antibody for either 2 hours at room temperature or overnight at 4ºC. After

washing in phosphate buffer saline (PBS), the specimens were incubated with Vector ImmPress detection kit corresponding to the primary antibody's host and counterstained with hematoxylin. For the double stain with β-amyloid and GFAP, antigen retrieval was performed with Dako target retrieval solution (a modified citrate buffer from Dako, Carpinteria, CA), steaming for 25 minutes, and then treated with peroxidase blocking buffer as above, and endogenous biotin blocked with Vector Avidin/Biotin blocking kit (Vector, Burlingame, CA). Staining for β-amyloid was done with the mouse-on-mouse peroxidase kit according to the manufacturer's instructions (Vector Labs). Diaminobenzidine (DAB) was used for color labeling for β-amyloid (brown). For GFAP immunostaining, Dako's streptavidin phosphatase kit was used with permanent red (red) as the chromophore.

Qualitative Detection

Morphology and histology were interpreted by an ophthalmic pathologist (masked for specific study groups) on H&E slides. Immunostained slides were evaluated for positivity of stain in a graded scale from 0 to 3+, where 0 indicated absence of staining and 3+ indicated marked positivity and more than 3 positive cells per layer. Immunoreactivity was evaluated in the corneal epithelium and endothelium, iris, lens, choroid, retinal ganglion cell (RGC) layer, inner nuclear layer (INL), outer nuclear layer (ONL), and optic nerve.

Quantitative Detection

To quantify oxidative-related DNA damage in the retina, densitometric quantification of 8OHdG immunohistochemistry was performed. Briefly, digital color images of the retina were processed using NIH ImageJ ver.1.68 (Abramoff *et al.*, 2004) and converted to an 8-bit inverted gray-scale image for analysis. Regions of interest were selected from each retina section, corresponding to the RGC, INL, and ONL as well as nearby areas without immunoreactivity for background measurements. Five sections were analyzed for each sample, for which the mean density per unit area (minus mean background density) was measured.

To quantify apoptosis in the retina, activated caspase-3 positive cells were identified for each

retinal sample and expressed over the total number of cells in each of the following retinal layers: RGC, INL, and ONL. Cellular number was determined with the cell counting plug-in for ImageJ ITCN (Byun et al., 2006).

Gene Expression Analysis

Mouse retina was microdissected and placed in RNAlater (Life Technologies, Grand Island, NY). Total RNA was then isolated using the AllPrep DNA/RNA Micro kit (Qiagen, Valencia, CA) and analyzed for quality using an Agilent 2100 Bioanalyzer. All samples used reported a RNA Integrity Number (RIN) >7.0. The Quantitect Reverse Transcriptase kit (Qiagen) was then used to generate cDNA templates for subsequent real-time qPCR analysis. Fifty nanograms of RNA were used in each reverse transcriptase reaction in a total reaction volume scaled to 30 μL according to manufacturer's instructions, and the synthesis reaction was allowed to proceed for 2.5 hours. qPCR amplifications were done in a total volume of 20 μL using 1 μL of a 1:10 dilution of the cDNA pool obtained in the previous step and SYBR Green qPCR mastermix (BioRad, Hercules, CA) on a Bio-Rad CFX96 real-time PCR detection system. Samples were run in three technical replicates each. Primers (Qiagen) were selected to hybridize with genes specific for various cellular response pathways according to relevant findings in the literature that reported known roles in retinal stress, degeneration, oxidative stress, inflammation, and death/survival (Table 1). Three housekeeping genes (Hprt1, Rplp0, and Rpl13) were selected according to previously reported expression stability (van Wijngaarden et al., 2007). Normalization to the housekeeping genes was performed using the geNorm algorithm (Vandesompele et al., 2002) built into the CFX96 software, which computes a normalization factor for each sample from the contribution of each housekeeping gene.

RESULTS

Histological Analysis of Eye Specimens

Results are summarized in Table 2. All groups showed corneal acanthosis, defined as thickening of the epithelium of more than 5 layers of cells, and edema defined as clearing of cytoplasm with enlargement of the cell. However, irregular acanthosis, irregular increment of cell layers, with pronounced edema was present in the VIV group at R+7 (mice #41, 42). All mice had inflammatory cells either in the anterior chamber or vitreous, regardless of the group. Focal cortical cataracts, disrupted fibers, and formation of globules in the cortex of the lens, which is located between the nucleus and the epithelium, were present in several mice. As shown in Figure 1, full cortical cataracts were seen only in the two mice of the FLT group at R+7 group and this was associated with caspase-3 2+ staining. The VIV group at R+7 had no morphologic changes of cataract but had caspase-3 2+ staining as well (see below). Apoptosis of neurons defined as shrinkage of the cytoplasm with hyperchromatic nuclei and degenerated chromatin was observed in some mice. These findings were quantified using immunohistochemistry and they are discussed below. Some slides showed artifacts in the histology (possibly due to traumatic enucleation) that precluded complete interpretation. These findings are not included in the interpretation. Only those findings that are clear and not affected by processing are reported.

Oxidative Stress: 8OHdG

Cornea

8OHdG immunoreactivity was positive in all mice in the acanthotic areas of the cornea. In the FLT group, positivity was evidenced in the corneal epithelium and endothelium, but we were not able to document significant differences compared to AEM and VIV controls with the present data.

Retina and Optic Nerve

Figure 2 summarizes 8OHdG data. The two mice in the FLT group at R+1 showed frank positivity for 8OHdG in the neuronal layer. One of these also evidenced 8OHdG in some vessels over the ON head. Digital quantitative analysis of immunoreactivity in the retinal layers was more prominent in the RGC of FLT samples at R+1 (Figure 2B). Comparing FLT samples at the different tissue collection time points, 8OHdG immunoreactivity decreased from R+1 to R+7 (Figure 2B, C, D, and E). All mice were negative at the level of the optic nerve.

Table 1. Genes of interest evaluated for expression changes in the mouse retina. Grouping was done according to relevant cellular processes and complete gene name with gene symbol are provided, as well as references reporting possible relevant roles in retina physiology.

Process	Gene Symbol	Gene name
Cell death and survival **(Lohr et al., 2006)**	Bax	Bcl2-associated X protein
	Bcl2	B-cell lymphoma 2[1]
	Bag1	Bcl2-associated athanogene 1[2]
	Atg12	Autophagy related 12[3]
Cellular Stress response	Hsf1	Heat shock transcription factor 1
	Hspa1a	Heat shock 70kDa protein 1A[4]
	Sirt1	Sirtuin 1[5]
	Nfe2l2 (Nrf2)	Nuclear factor (erythroid-derived 2)-like 2[6]
Oxidative stress response	Hmox1	Heme-oxygenase 1[7]
	Cat	Catalase
	Sod2	Superoxide dismutase 2, mitocondrial[8]
	Gpx4	Glutathione peroxidase 4[9]
	Prdx1	Peroxiredoxin 1
	Cygb	Cytoglobin
Inflammation	Nfkb1	Nuclear factor of kappa light polypeptide gene enhancer in B-cells 1[10]
	Tgfb1	Transforming growth factor beta 1[11]
Normalizing genes	Rpl13	Ribosomal protein L13
	Rplp0	Ribosomal protein, large, P0
	Hprt	hypoxanthine phosphoribosyltransferase 1

1 (Godley et al., 2002)   5 (Chen et al., 2009)   9 (Ueta et al., 2012)
2 (Liman et al., 2008)   6 (Wei et al., 2011)   10 (Wise et al., 2005)
3 (Wang et al., 2009)   7 (Zhu et al., 2007)   11 (Gerhardinger et al., 2009)
4 (Awasthi and Wagner, 2005)   8 (Justilien et al., 2007)

Apoptosis: Caspase-3

Cornea

Activated caspase-3 appeared positive in the cornea of all mice with the same intensity.

Lens

Two mice of the FLT group at R+7 had cataract formation associated with caspase-3 2+ staining (Figure 1). The VIV group at R+7 had no morphologic changes of cataract but had caspase-3 2+ staining as well.

Retina and Optic Nerve

Detection of apoptosis by activated caspase-3 immunoreactivity was performed on retinal sections and compared in the different specimens (Figures 1 and 3). All mice showed positivity in the neuronal layer regardless of day of sacrifice. Digital image quantification of caspase-3 immunoreactivity revealed that VIV samples had the highest percentage of apoptotic cells in the INL and RGC layer, followed by FLT samples, at day R+1 and R+7. Comparatively, VIV and FLT retina samples showed more caspase-3 positive

Table 2. Histologic interpretation with Hematoxylin-Eosin. Data arranged according to group (FLT, AEM, VIV) and day of sacrifice: 2 mice per group at R+1, +5, or +7, respectively.

	Cornea			Lens			Retina			ON		
	FLT	AEM	VIV	FLT	AEM	VIV	FLT	AEM	VIV	FLT	AEM	VIV
Day 1	FA and E	FA	FA	Anterior subcapsular C	Nml	Anterior subcapsular C	Nml	Nml	Nml	Nml	Nml	Nml
	Bullae*, A 1+, E 2+ basal layer calcification	A* 2+	FA	Nml	Nml	Anterior subcapsular C	Nml	Nml	Nml	Nml	-	Nml
Day 5	FA and basal E	FA*, E 1+	Central E	Nml	Focal cortical C	Nml	Nml	Nml	Nml	Nml	Nml	Nml
	FA	Intranuclear inclusions, A 1+, E 2+	FA	Nml	Focal cortical C	Anterior subcapsular C	Nml	Nml	Nml	Nml	Nml	Nml
Day 7	FA	FA	Irregular A 1+ E 3+	Cortical C	Nml	Nml	Nml	Nml	Nml	Nml	Nml	Nml
	A* 1+, E 2+	FA	Irregular A 1+ E 2+	Cortical C	Nml	Nm	Nml	Nml	Nml	Nml	Nml	Nml

(A)= acanthosis, (C)= cataract, (E)= edema, (FA)= focal acantosis, (Nml)=normal, anterior subcapsular C (anterior subcapsular cataract is disruption of the fibers with proliferation of the epithelium in the anterior subcapsular áreas of the lens)
Comments: *Anterior chamber 1+ cell

cells than AEM samples at R+1, except for the INL in the AEM group at R+7. VIV samples also tended to increase their percentage of apoptotic cells at day R+7, as seen in qualitative analysis. Retinal pigment epithelium (RPE) of the FLT group at R+1 and one mouse at R+5 showed positivity with caspase-3, and one mouse AEM R+7 showed only rare and focal RPE staining (Figure 1). Qualitative and quantitative evaluation of ON immunoreactivity was inconclusive.

β-amyloid and GFAP

β-amyloid and GFAP stains were studied in the retina and optic nerve only and immunostained retina sections are shown in Figure 4. With regard to the retina, all mice were positive in the neuronal layer for β-amyloid. Overall, the vivarium mice showed a slightly higher positivity in both RGC and INL compared to the rest of the mice (VIV animals showed 2-3+ positivity at R+1 and R+5, more than any other group; one FLT animal at R+7 showed similar 2+ reactivity). GFAP was present in astrocytes of the retinal neuronal layer in at least one mouse of each group, except in the FLT group at R+5, where it was absent. No activation (positivity) of Muller cells was noted in any of the eyes.

While results were not conclusive from these retinal findings, it is important to note that only the FLT group at R+1 were positive for all stains

at the retinal neuronal layer: 8OHdG, caspase-3, β-amyloid, and GFAP.

At the level of the optic nerve, only the FLT group at R+7 showed positivity for both β-amyloid in the axons and GAFP in the astrocytes either at the level of the lamina cribrosa or distal to it (Figure 4). No co-expression was seen of GFAP and β-amyloid in same cell type.

Cellular Responses Identified by Gene Expression Analysis

Gene expression profiling on STS-133 flight samples and their AEM and vivarium ground controls was performed targeting a set of genes focused on cellular death and survival, oxidative stress and cellular stress response, and inflammation. Results are shown in Figure 5 and Figure 6 and expressed as comparative normalized expression across the individual specimens at R+1 and R+7 for all groups. Due to the limited sample size, statistical analysis was not possible and these results are mainly descriptive.

Activation of Oxidative Stress Response and Pro-Inflammatory Genes

Figures 5 and 6 (see section below) plot gene expression data measured by real time qPCR. Several genes coding for key antioxidant enzymes (Hmox1, Sod2, Cat, Gpx4, Cygb, Prdx1) were elevated in retina samples obtained immediately after flight (Figure 5B), but this elevation returned

to levels closer to AEM ground control values at 7 days post-landing. A similar trend was observed for inflammatory mediators Nfkb1 and Tgfb1 (Figure 5A).

Hmox1 showed the highest levels in those samples for which a higher evidence of stress was observed (FLT samples at R+1 and VIV ground controls).
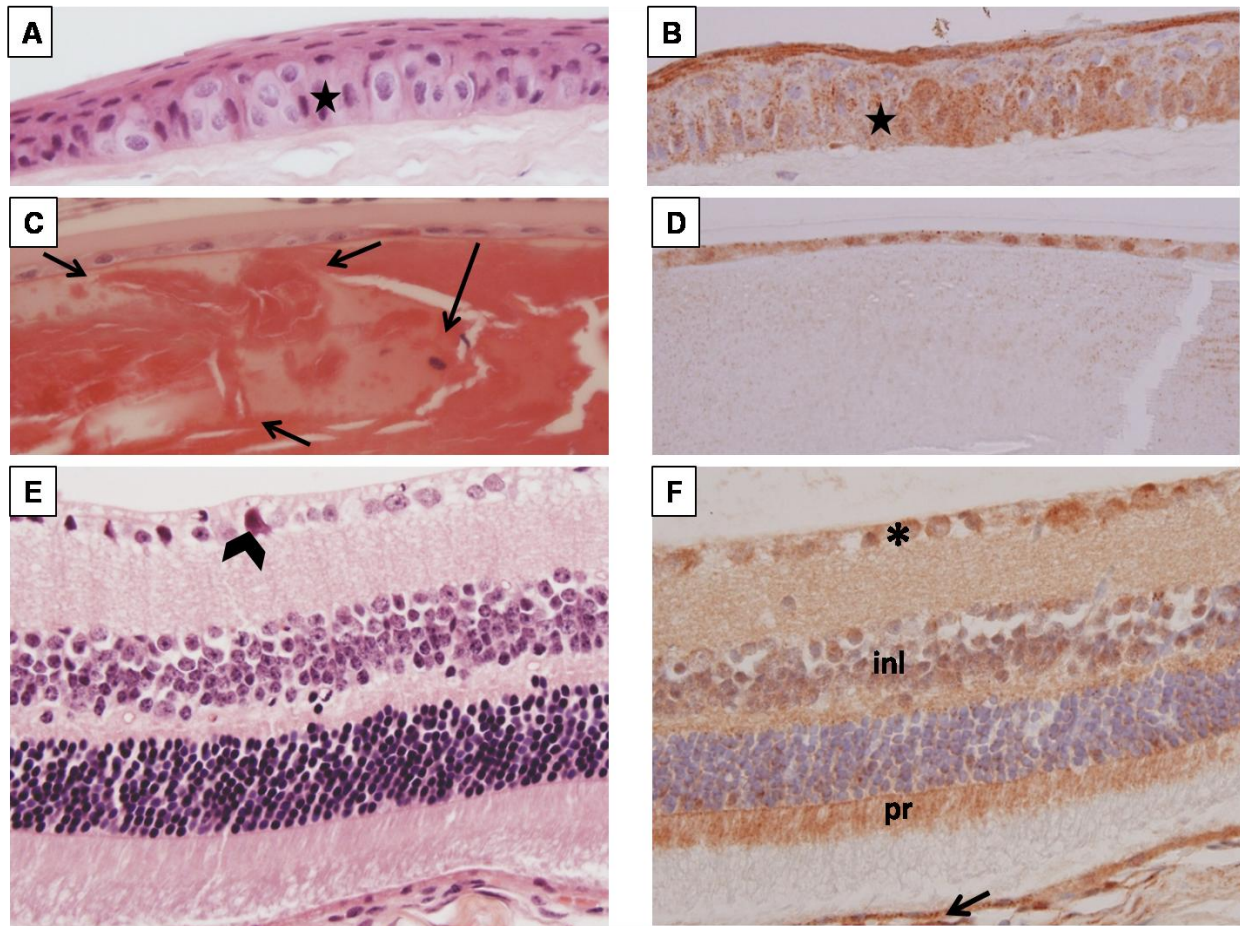

Figure 1. Histological analysis of H&E and Caspase-3 stained eye samples. Hematoxylin and Eosin stain, original magnification 20X : Panel A. AEM R+7, Epithelium of cornea showing focal edema of cells seen as clearing and enlargement of the cytoplasm in the basal layers (star marks the level of the basal layers) and acanthosis (thickening of more than 5 layers of cells). Panel C. FLT R+1, anterior lens with cortical cataract seen as disorganization of the fibers of the cortex (arrows at the level of the cortex). Notice the displaced nucleus (nucleus of epithelial cells of the lens should only be present in the subcapsular area and not in the cortex in the anterior portion of the lens). Panel E. FLT R+1, retina with an apoptotic neuron seen as a shrunken cell with hyperchromatic condensed nucleus and eosinophilic cytoplasm (arrow head). Remainder of retina appears morphologically unremarkable. Caspase 3 immunostaining: Panel B. FLT R+1 corneal epithelium staining positively with Caspase 3 in the superficial layers and in the basal layers (star). Positive staining of the basal cells of the corneal epithelium is seen in the focal acanthotic areas, and in the upper differentiated layers (internal positive control). Panel D. FLT R+1 lens epithelium staining with Caspase 3; notice that cortex is negative. Panel F. FLT R+1, retina with caspase-3 staining of cytoplasm of neurons (*) predominantly with faint staining of the inner nuclear layer (inl) and inner segments of photoreceptors (pr). The cytoplasm of RPE cells is also staining (arrow).
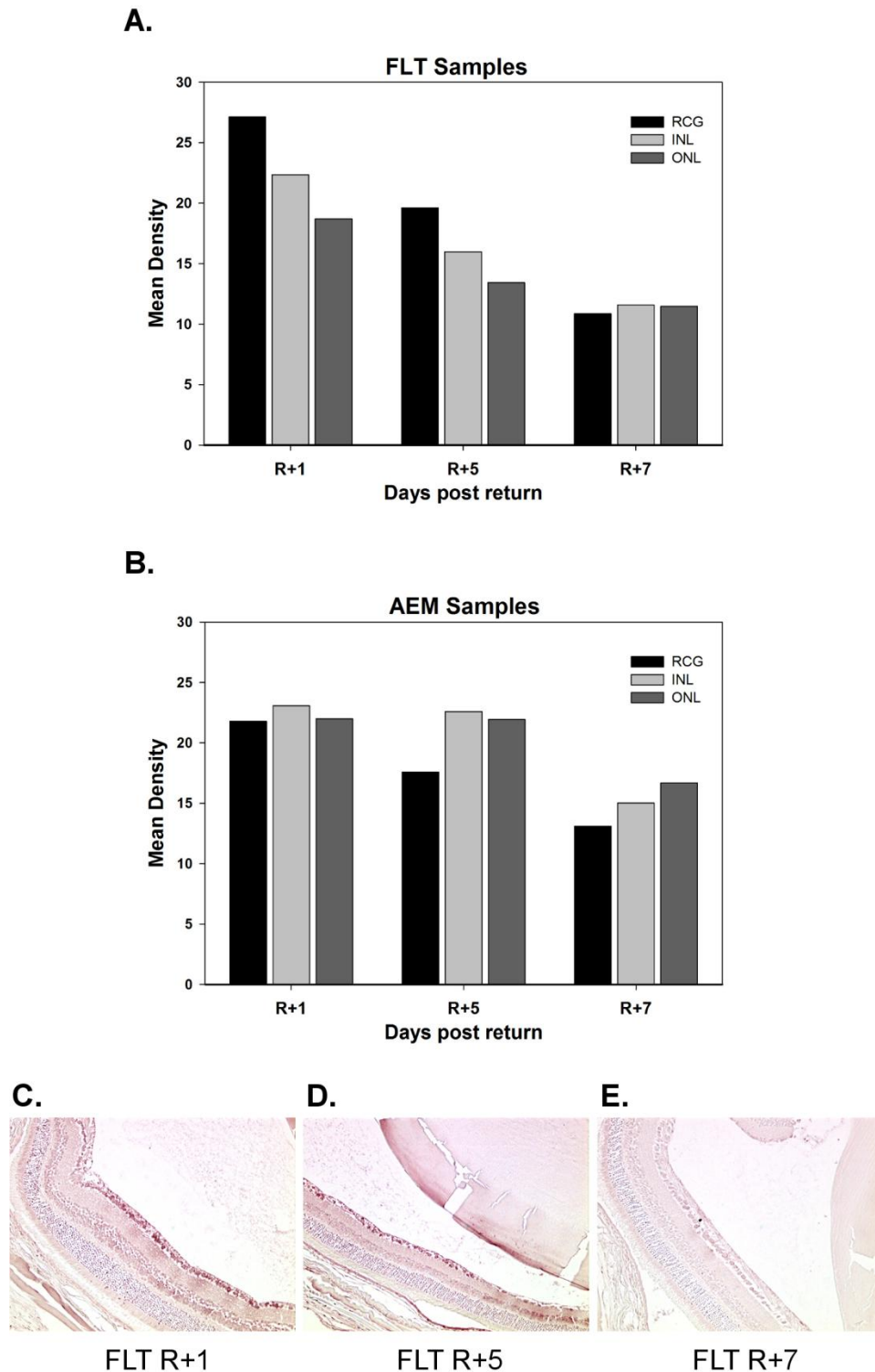
Figure 2. 8OHdG immunoreactivity in retinal neuronal layers of AEM and FLT mice. Bars indicate the mean of n=2 biological samples. Each individual neuronal cell layer was compared at R+1, R+5, and R+7 in AEM samples (panel A) and Flight samples (panel B). Representative images of 8OHdG stained histological sections of the retina in FLT samples at R+1 (panel C), R+5 (panel D), and R+7 (panel E).
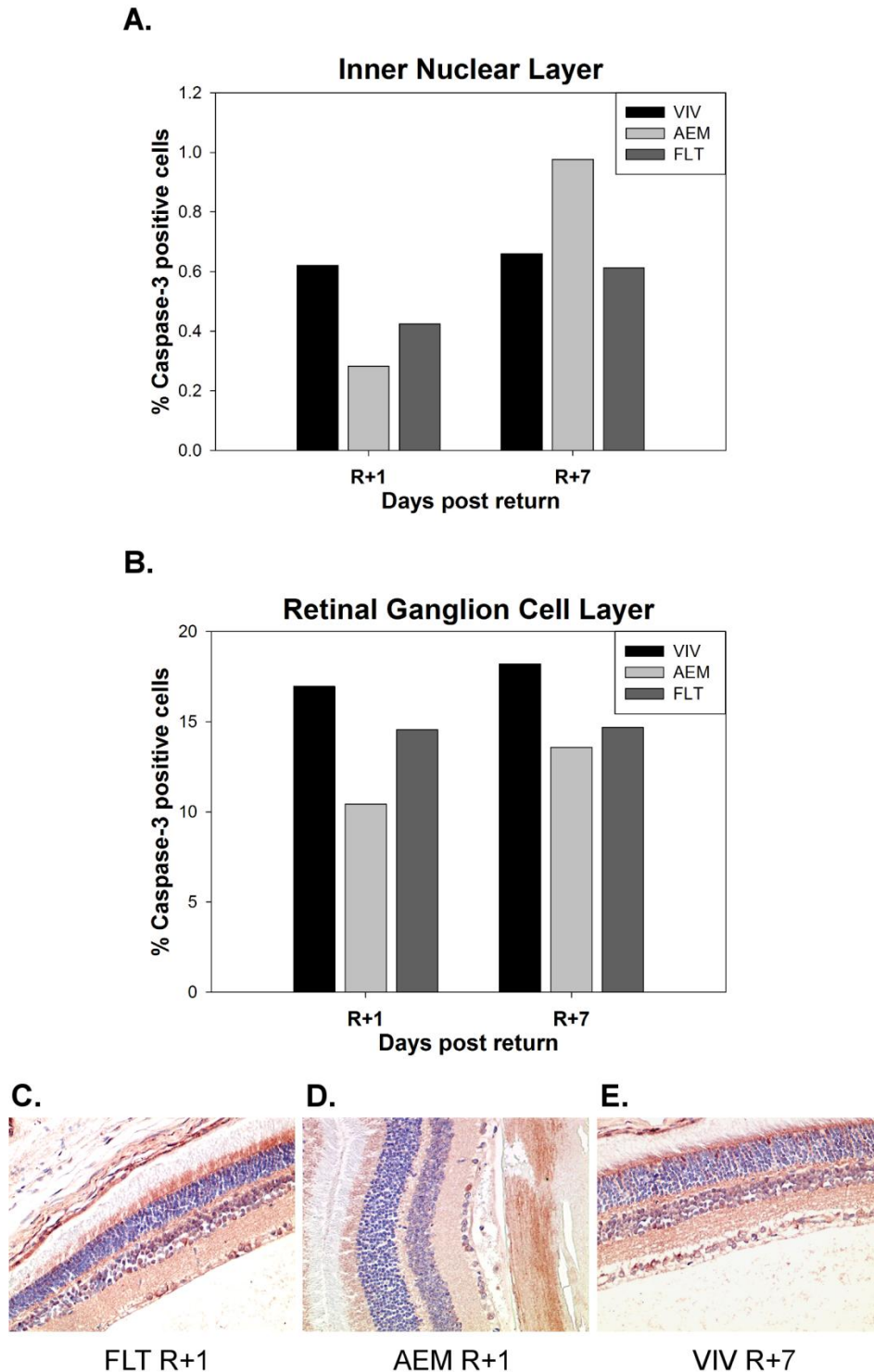
A.

B.

C.   **D.**   **E.**

FLT R+1   AEM R+1   VIV R+7

Figure 3. Quantification of Caspase-3 immunoreactivity by neuronal layer. Percentage of caspase-3 positive cells in the Inner Nuclear Layer (panel A) and the Retinal Ganglion Cell Layer (panel B) was calculated as described in Methods for day R+1 and R+7 tissue collection time points. Representative images of histological sections stain (red-brown) for caspase-3 of Flight (panel C), AEM (panel D), and Vivarium (panel E) samples at day R+1. Arrows indicate caspase-3 positive stained cells identified in different layers of the retina.
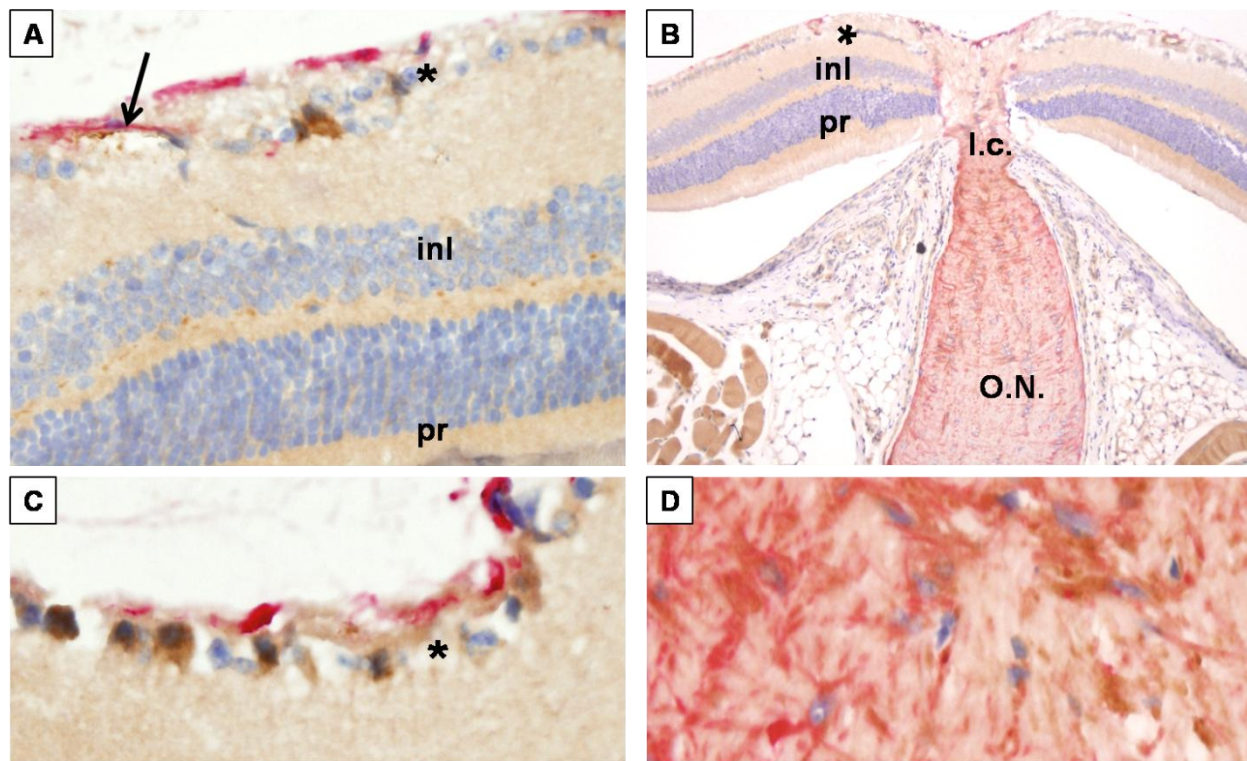
Figure 4. Beta amyloid (brown) and glial fibrillary acid protein (GFAP) (red) double staining immunohistochemistry. A: FLT R+1 (mouse #13). Retina with focal positive cytoplasmic staining in neurons of the ganglion cell layer (*) with β-amyloid (brown). Perivascular (arrow) and other astrocytes in the ganglion cell layer stain with GFAP (red). Notice the negative staining of Muller cells with GFAP. B: FLT R+1 optic nerve. Note the staining of the optic nerve (O.N.) in the region posterior to the lamina cribrosa (l.c.) with GFAP and focally with β-amyloid. Non-specific staining of the orbital muscle is also seen with β-amyloid (brown). C: FLT R+1 retina higher magnification of focal positivity with β-amyloid (brown) in ganglion cell layer (*) and GFAP in astrocytes (red). D: FLT R+1 optic nerve higher magnification of immediate post-laminar region. Notice the staining of oligodendrocytes and astrocytes with GFAP (red) and the β-amyloid stain (brown) of the nerve fibers in between the glial cells.
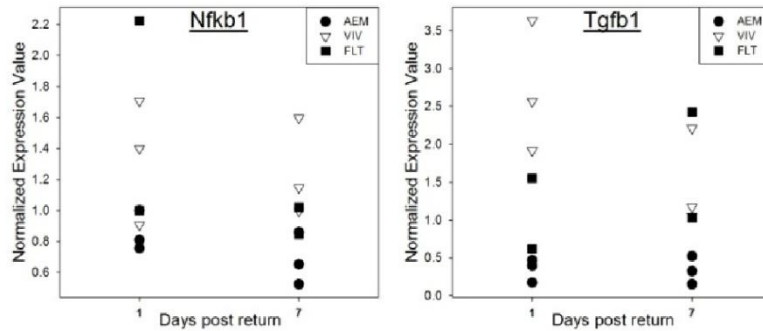
Cell Death and Survival Genes

The proapoptotic gene Bax was elevated in one flight sample (#13) at day R+1 and moderately elevated in one flight sample (#52) at R+7. Vivarium mice showed a higher expression of Bax at all collection time points compared to AEM ground controls. FLT samples at R+1 and VIV samples exhibited higher levels of the autophagy marker Atg12 and the survival genes Bcl2 and Bag1, suggesting that cellular protection mechanisms may be triggered as a response to cellular stress (Figure 6A).

Activation of Cellular Stress Genes

The cellular stress response genes Hsf1and Nrf2 (Nfe2l2) were expressed slightly higher in VIV samples compared to AEM controls. Among the FLT mice, there was a tendency to higher expression at R+1 than R+7 (Figure 6B). The Hsf1 activator sirtuin 1 (Sirt1) did not show major differences across the various samples. Interestingly, the heat shock protein 70KDa Hsp1a1 was expressed at a lower level in mouse #13 that exhibited, overall, the highest signs of stress.

A. Inflammatory Response Genes

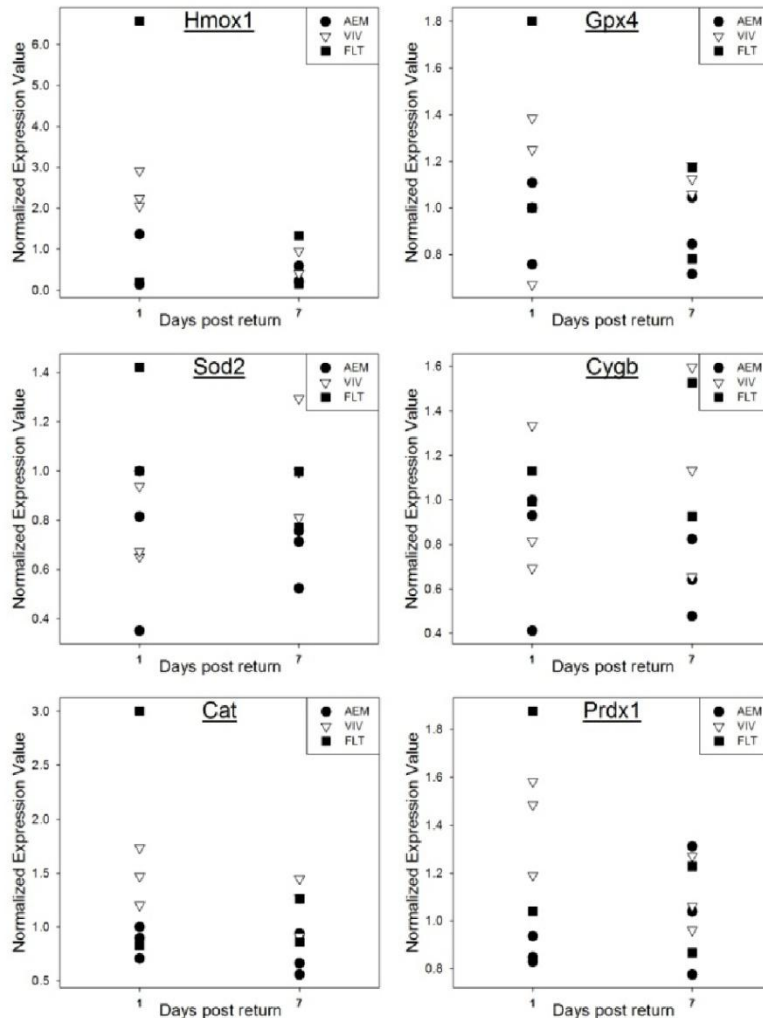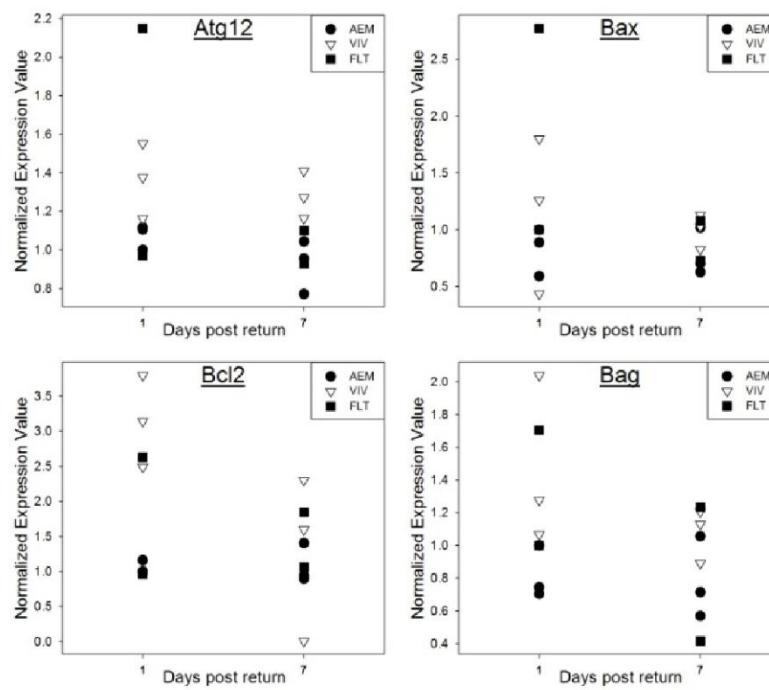## B. Oxidative Stress Response Genes

Figure 5. Gene expression analysis of inflammatory and oxidative stress response genes. Inflammatory response (panel A) and oxidative stress (panel B) gene expression levels from RNA isolated from retina samples in Flight (FLT), AEM, and Vivarium (VIV) samples at day R+1 and R+7, measured by real time qPCR. Y axis represents the comparative gene expression levels normalized to housekeeping genes.
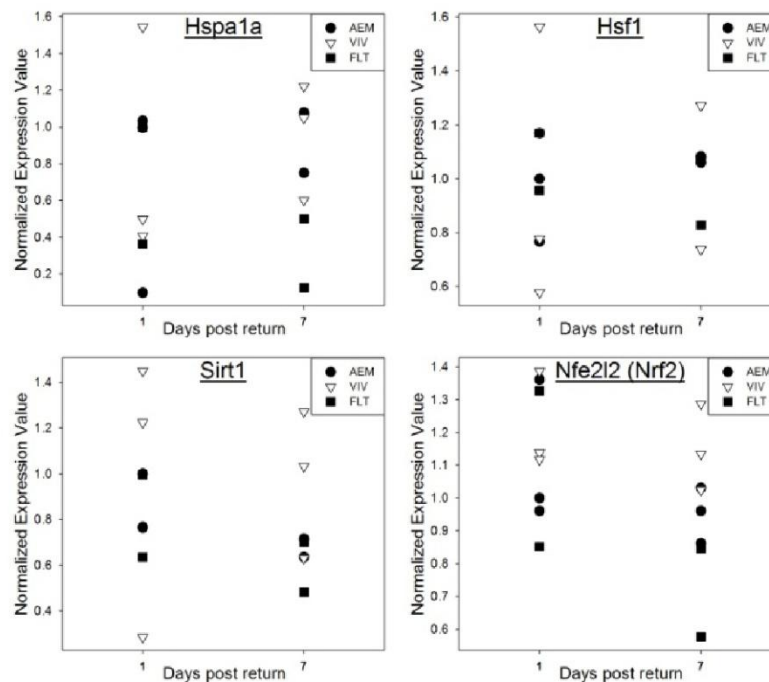
Figure 6. Gene expression analysis of cell death and survival and cellular stress response genes. Cell death and survival (panel A) and cellular stress (panel B) gene expression levels from RNA isolated from retina samples in Flight (FLT), AEM, and Vivarium (VIV) samples at day R+1 and R+7, measured by real time qPCR. Y axis represents the comparative gene expression levels normalized to housekeeping genes.

DISCUSSION

While the spaceflight results reported herein represent pilot data due to the small sample size, these data offer, for the first time, direct evidence suggesting that oxidative stress, neuronal damage, and mechanical injury take place in the retina, lens, and optic nerve of rodents flown in low-Earth orbit for a period under two weeks. Several previous studies have shown the occurrence of oxidative stress during spaceflight (Stein, 2002), however, our work gives a first insight into the impact of space-associated factors on biological processes like cell death, oxidative stress, and probable mechanical injury in the rodent eye.

Because the BALB mouse strain used in the STS-133 experiment is susceptible to light-induced retinal degeneration (LaVail et al., 1987), we speculate that this particular strain exhibits an enhanced sensitivity to oxidative stress and/or a reduced stress response, making it a suitable strain in which to identify alerting evidence of risks previously unrecognized in the retinal tissue, while impacting its value as a model for the study of the human changes seen in-flight.

8OHdG, a product of deoxyguanosine oxidation, is a marker of oxidative stress-induced DNA damage. This damage has been observed in mouse cornea exposed to dryness (Nakamura et al., 2007), ultraviolet radiation (Tanito et al., 2003), and in mouse retina exposed to intense light (Tanito et al., 2002; Wiegand et al., 1983). In our study, 8OHdG was present in all acanthotic areas of the cornea. Irregular acanthosis with visible edema was only seen in the VIV samples at R+7, and it was only in this group where positivity at the corneal endothelium was observed since day 1, suggesting an impaired ion and water transport in the cornea.

The retinal response to intense light in susceptible mice has been studied before and has been found to be related to lipid peroxidation at the ONL (Tanito et al., 2002; Wiegand et al., 1983). Likewise, radiation-induced retinopathy is an ocular complication in cancer patients that receive radiation therapy (Parsons et al., 1996). The processes involved in the damage by high-energy-particle radiation in these cases may share commonalities (direct DNA damage and oxidative stress) with exposure to radiation present during spaceflight. The present work shows evidence of both oxidative stress-induced DNA damage in the neuronal layers of flight mice retinas and of an oxidative stress response induced at the gene expression level in these mice. Short-term responsiveness to DNA oxidation followed by DNA repair has been studied longitudinally in blood of trauma patients (Oldham et al., 2002), suggesting that the attenuated DNA damage observed after one week of return from flight may be the result of DNA repair.

Of note, the ground controls kept in the vivarium exhibited a comparable level of retinal oxidative stress to the samples from flight, especially at longer exposures (day R+7). This is likely due to the fact that the illumination conditions in a standard vivarium room are approximately 15-fold in light flux compared to the illumination of an AEM, even if both maintain a 12 hour light-12 hour dark cycle.

Caspase-3 is a pro-enzyme that is activated in the intrinsic apoptotic pathway in all mammals (D'Amelio et al., 2010). In this study, all mice showed positivity for caspase-3 at the level of the cornea. This may be explained by the fact that caspase-3 immunoreactivity in the stratified epithelium of the cornea serves as an internal positive control due to the natural differentiation process that the basal cells suffer towards cornification. Apoptosis can be triggered by oxidative stress, brain trauma, or ischemia. In a model of brain ischemia, the area of neuronal apoptosis has been identified not in the infarct region but in the surrounding area, where the oxygen tension is decreased, but not absent (Pulsinelli et al., 1982). The presence of activated caspase-3 is thus related to hypoxic environment and radiation exposure. In our study, the FLT group at R+1 showed higher positivity compared to the rest of the groups. This may be related to radiation and microgravity exposure during spaceflight. It is important to point out that the effect of high-energy-particle radiation may be overall increased in this susceptible mouse strain.

Qualitative examination revealed that VIV and FLT groups showed more caspase-3-positive cells at the retinal layers than AEM retinas. This may suggest that the damage caused by visible light radiation in the albino strain in the vivarium conditions may be comparable to the damage caused by the exposure to spaceflight

environmental factors. We also observed positive microglial (astrocytes) but not Muller cell activation in VIV specimens, which may support the notion of visible light radiation effects as the triggering factor in inner layers of the retina only in these mice (Song et al., 2012).

Both mice in the FLT group at R+1 and one mouse at R+5 showed evidence of apoptosis in the RPE. Apotosis in the RPE has been identified in ocular pathologies like age-related macular degeneration (AMD) secondary to exposure to activated monocytes (Yang et al., 2011), or triggered by oxidative stress with H_2O_2, lipofuscin, or light irradiation (Sparrow et al., 2000). This data also suggest oxidative stress may be an important component in the retinal damage in these mice. Of note, in vitro experiments with human RPE cells cultured in simulated microgravity generated by a NASA-bioreactor resulted in DNA damage and inflammatory response in these cells (Roberts et al., 2006). Retinal pigment epithelium attenuation has been related to retinal choroidal folds previously found in astronauts (Mader et al., 2011). It is yet to be determined whether or not increased RPE apoptosis may contribute to the formation of choroidal folds or if it increases the risk for AMD in astronauts.

Several advances in immunohistochemistry have led to the identification of β-amyloid in traumatic brain injury in humans (Iwata et al., 2002), rats, and pigs (Smith et al., 1999), by tracing not only the full-length protein but also small aminoacid peptides. β-amyloid was present in areas of the brain as soon as one day after brain trauma was provoked by pressure injection of saline into the cranium in a rat model (Pierce et al., 1996). Moreover, β-amyloid deposits showed evidence of optic nerve injury in cases of shaken-baby syndrome (Gleckman et al., 2000). Previous studies in animal models have shown distribution of β-amyloid in the mouse retina that suggests its involvement in the pathophysiology of glaucoma (Kipfer-Kauer et al., 2010). We report that β-amyloid deposition was present in the neural retina of mice in all treatment groups and that the VIV mice showed a slightly higher positivity in both RGC and INL compared to the rest of the mice. Interestingly, β-amyloid was present in the optic nerve of both mice in the FLT group at R+7

and had the unique characteristic of being at the level of lamina cribrosa or immediately distal to it. This compares with the findings in traumatic injury in children of shaken-baby syndrome where most of the axonal changes are seen in the postlaminar region (Gleckman et al., 2000). This may be associated to the anatomy of this region where the nerve is anchored by the fibers of the lamina cribrosa but immediately posterior to this or beyond this area the nerve can move freely. Thus, in the event of mechanical trauma the immediate fibers in the postlaminar region may be the ones demonstrating more damage. The trauma may include increased intracranial pressure that is transmitted into the nerve, positional or whiplash (similar, although in a less intense manner to what happens in shaken baby syndrome), or vibration (as the one occurring during launch or landing). However, there is the need to further investigate the nature of the changes through additional experimental work.

GFAP is an intermediate filament protein known to be present in astrocytes, Muller cells, and oligodendrocytes in the post-laminar optic nerve. GFAP is elevated when there is stress in the central nervous system and has been shown in the injured retina mostly present in the activated Muller cells (Lewis and Fisher, 2003). In this paper, we show that the optic nerves of several mice were positive for GFAP and β-amyloid; however, it was only the FLT group at R+7 that showed increased expression of GFAP at the postlaminar optic nerve. These findings suggest that the astrocytes and oligodendrocytes were activated in this region probable secondary to mechanical trauma. The causes of this, either vibration or fluid shift-related, need to be further investigated.

In addition, only FLT mice sacrificed at day 1 (FLT R+1) were immunoreactive in the neuronal layer for all β-amyloid, GFAP, caspase-3, and 8OHdG, suggesting increased oxidative and possibly mechanical damage. This may be explained by the possible correlation of β-amyloid deposition and activation of astrocytic cells, both triggering reactive oxygen species production (Lamoke et al., 2012).

The gene expression profiling results with BALB mice in flight STS-133 support the immunohistopathologic findings and suggest that:

a) Oxidative stress-induced DNA damage was higher in the FLT samples compared to controls on R+1, and decreased on R+7. A trend toward higher oxidative and cellular stress response gene expression was also observed on R+1 compared to AEM controls, and these levels decreased on R+7. Several genes coding for key antioxidant enzymes, namely, heme-oxygenase-1, peroxiredoxin, and catalase, were among those elevated after flight. Likewise, the inflammatory response genes Nfkb1and Tgfb1 were elevated after flight. The fact that only two mice flown on STS-133 were genetically analyzed per day of sacrifice creates a major limitation in any statistical analysis. However, this does not preclude the comparisons of samples. b) There is an apparent correlation trend in the stress parameters measured in the different animals and there is certain variability in the stress response among the individual animals. For example, mouse # 13 in the FLT group at R+1 suffered from overall elevated stress, demonstrated by the highest 8OHdG levels, induction of antioxidant enzymes, induction of Nfkb1, and concomitant lower levels of the cytoprotective heat shock protein Hsp1a1. Sirtuin 1 gene expression results were non-conclusive, but further analysis is required to determine if translocation of sirtuin 1 may occur and how this may affect the expression of downstream cellular stress response genes (Jaliffa *et al.*, 2009; Ozawa *et al.*, 2010). c) Spaceflight represents a source of environmental stress that translates into oxidative and cellular stress in the retina, which is partially reversible upon return to Earth. Also, retinas from VIV control mice evidenced higher oxidative stress markers, Nfkb1 and Tgfb1, likely due to the more intense illumination in vivarium cages versus the AEM.

In addition, mice in FLT group at R+7 were positive for both β-amyloid and GFAP, and it was only in these mice that there was increase in GFAP staining adjacent to lamina cribrosa in the optic nerve. We suspect some long term damage in the optic nerve may be seen after spaceflight because this did not resolve after seven days on Earth. Additional quantitative experiments are needed to give a better understanding on this finding.

These preliminary data suggest that spaceflight represents a source of environmental stress that directly translates into oxidative and cellular stress in the retina, which is partially reversible upon return to Earth. Moreover, the optic nerve findings suggest that the lesion may be mechanical in nature and that does not resolve after return to Earth, at least in the animals studied. Further work is needed to dissect the contribution of the various spaceflight factors (microgravity, radiation) and to evaluate the impact of the stress response on retinal and optic nerve health. These preliminary results should inform investigators on the design of future studies utilizing a more suitable mouse strain devoid of photic degeneration predisposition, male animals that better reflect the astronaut population, and statistically powered larger sample sizes.

ACKNOWLEDGEMENTS

REFERENCES

Abramoff, M.D., Magalhaes, P.J., and Ram, S.J. 2004. Image processing with ImageJ. *Biophotonics International.* 11: 36-42.

Awasthi, N. and Wagner, B.J. 2005. Upregulation of heat shock protein expression by proteasome inhibition: an antiapoptotic mechanism in the lens. *Investigative Ophthalmology & Visual Science*. 46: 2082-2091.

Byun, J., Verardo, M.R., Sumengen, B., Lewis, G.P., Manjunath, B.S., and Fisher, S.K. 2006. Automated tool for the detection of cell nuclei in digital microscopic images: application to retinal images. *Molecular Vision*. 12: 949-960.

Chen, D., Pacal, M., Wenzel, P., Knoepfler, P.S., Leone, G., and Bremner, R. 2009. Division and apoptosis of E2f-deficient retinal progenitors. *Nature*. 462: 925-929.

Cucinotta, F.A., Manuel, F.K., Jones, J., Iszard, G., Murrey, J., Djojonegro, B., and Wear, M.

2001. Space radiation and cataracts in astronauts. *Radiation Research*. 156: 460-466.

D'Amelio, M., Cavallucci, V., and Cecconi, F. 2010. Neuronal caspase-3 signaling: not only cell death. *Cell Death & Differentiation*. 17: 1104-1114.

Friedman, D.I. 2007. Idiopathic intracranial hypertension. *Current Pain and Headache Reports*. 11: 62-68.

Frigeri, A., Iacobas, D.A., Iacobas, S., Nicchia, G.P., Desaphy, J.F., Camerino, D.C., Svelto, M., and Spray, D.C. 2008. Effect of microgravity on gene expression in mouse brain. *Experimental Brain Research*. 191: 289-300.

Gerhardinger, C., Dagher, Z., Sebastiani, P., Park,Y.S., and Lorenzi, M. 2009. The transforming growth factor-beta pathway is a common target of drugs that prevent experimental diabetic retinopathy. *Diabetes*. 58: 1659-1667.

Gleckman, A.M., Evans, R.J., Bell, M.D., and Smith, T.W. 2000. Optic nerve damage in shaken baby syndrome: detection by beta-amyloid precursor protein immuno-histochemistry. *Archives of Pathology & Laboratory Medicine*. 124: 251-256.

Godley, B.F., Jin, G.F., Guo, Y.S, and Hurst, J.S. 2002. Bcl-2 overexpression increases survival in human retinal pigment epithelial cells exposed to H(2)O(2). *Experimental Eye Research*. 74: 663-669.

Hargens, A.R. and Watenpaugh, D.E. 1996. Cardiovascular adaptation to spaceflight. *Medicine and Science in Sports and Exercise*. 28: 977-982.

Iwata, A., Chen, X.H., McIntosh, T.K., Browne, K.D., and Smith, D.H. 2002. Long-term accumulation of amyloid-beta in axons following brain trauma without persistent upregulation of amyloid precursor protein genes. *Journal of Neuropathology & Experimental Neurology*. 61: 1056-1068.

Jaliffa, C., Ameqrane, I., Dansault, A., Leemput, J., Vieira, V., Lacassagne, E., Provost, A., Bigot, K., Masson, C., Menasche, M., and Abitbol, M. 2009. Sirt1 involvement in rd10 mouse retinal degeneration. *Investigative Ophthalmology & Visual Science*. 50: 3562-3572.

Justilien, V., Pang, J.J., Renganathan, K., Zhan, X., Crabb, J.W., Kim, S.R., Sparrow, J.R., Hauswirth, W.W., and Lewin, A.S. 2007. SOD2 knockdown mouse model of early AMD. *Investigative Ophthalmology & Visual Science*. 48: 4407-4420.

Kipfer-Kauer, A., McKinnon, S.J., Frueh, B.E., and Goldblum, D. 2010. Distribution of amyloid precursor protein and amyloid-beta in ocular hypertensive C57BL/6 mouse eyes. *Current Eye Research*. 35: 828-834.

Kramer, L.A., Sargsyan, A.E., Hasan, K.M., Polk, J.D., and Hamilton, D.R. 2012. Orbital and intracranial effects of microgravity: findings at 3-T MR imaging. *Radiology*. 263(3): 819-27.

Lamoke, F., Ripandelli, G., Webster, S., Montemari, A., Maraschi, A., Martin, P., Marcus, D.M., Liou, G.I., and Bartoli, M. 2012. Loss of thioredoxin function in retinas of mice overexpressing amyloid beta. *Free Radical Biology and Medicine*. 53: 577-588.

LaVail, M.M., Gorrin, G.M., and Repaci, M.A. 1987. Strain differences in sensitivity to light-induced photoreceptor degeneration in albino mice. *Current Eye Research*. 6: 825-834.

Lewis, G.P. and Fisher, S.K. 2003. Up-regulation of glial fibrillary acidic protein in response to retinal injury: its potential role in glial remodeling and a comparison to vimentin expression. *International Review of Cytology*. 230: 263-290.

Liman, J., Faida, L., Dohm, C.P., Reed, J.C., Bahr, M., and Kermer, P. 2008. Subcellular distribution affects BAG1 function. *Brain Research*. 1198: 21-26.

Lohr, H.R., Kuntchithapautham, K., Sharma, A.K., and Rohrer, B. 2006. Multiple, parallel cellular suicide mechanisms participate in photoreceptor cell death. *Experimental Eye Research*. 83: 380-389.

Mader, T.H., Gibson, C.R., Pass, A.F., Kramer, L.A., Lee, A.G., Fogarty, J., Tarver, W.J., Dervay, J.P., Hamilton, D.R., Sargsyan, A.,

Phillips, J.L., Tran, D., Lipsky, W., Choi, J., Stern, C., Kuyumjian, R., and Polk, J.D. 2011. Optic disc edema, globe flattening, choroidal folds, and hyperopic shifts observed in astronauts after long-duration space flight. *Ophthalmology*. 118: 2058-2069.

Naidu, S., Winget, C.M., Jenner, J.W., Mele, G., and Holley, D.C. 1995. Effects of housing density on mouse physiology and behavior in the NASA Animal Enclosure Module simulators. *Journal of Gravitational Physiology*. 2: 140.

Nakamura, S., Shibuya, M., Nakashima, H., Hisamura, R., Masuda, N., Imagawa, T., Uehara, M., and Tsubota, K. 2007. Involvement of oxidative stress on corneal epithelial alterations in a blink-suppressed dry eye. *Investigative Ophthalmology & Visual Science*. 48: 1552-1558.

NASA. 2010. *Longitudinal Study of Astronaut Health* database.

Oldham, K.M., Wise, S.R., Chen, L., Stacewicz-Sapuntzakis, M., Burns, J., and Bowen, P.E. 2002. A longitudinal evaluation of oxidative stress in trauma patients. *Journal of Parenteral and Enteral Nutrition*. 26: 189-197.

Ozawa, Y., Kubota, S., Narimatsu, T., Yuki, K., Koto, T., Sasaki, M., and Tsubota, K. 2010. Retinal aging and sirtuins. *Ophthalmic Research*. 44: 199-203.

Parsons, J.T., Bova, F.J., Mendenhall, W.M., Million, R.R., and Fitzgerald, C.R. 1996. Response of the normal eye to high dose radiotherapy. *Oncology*. 10: 837-847; discussion 847-838, 851-832.

Philpott, D.E., Corbett, R., Turnbill, C., Black, S., Dayhoff, D., McGourty, J., Lee, R., Harrison, G., and Savick, L. 1980. Retinal changes in rats flown on Cosmos 936: A cosmic ray experiment. *Aviation, Space, and Environmental Medicine*. 51: 556-562.

Philpott, D.E., Corbett, R., Turnbill, C., Harrison, G., Leaffer, D., Black, S., Sapp, W., Klein, G., and Savik, L.F. 1978. Cosmic ray effects on the eyes of rats flown on Cosmos No. 782, experimental K-007. *Aviation, Space, and Environmental Medicine*. 49: 19-28.

Pierce, J.E., Trojanowski, J.Q., Graham, D.I., Smith, D.H., and McIntosh, T.K. 1996. Immunohistochemical characterization of alterations in the distribution of amyloid precursor proteins and beta-amyloid peptide after experimental brain injury in the rat. *Journal of Neuroscience*. 16: 1083-1090.

Pietsch, J., Bauer, J., Egli, M., Infanger, M., Wise, P., Ulbrich, C., and Grimm, D. 2011. The effects of weightlessness on the human organism and mammalian cells. *Current Molecular Medicine*. 11: 350-364.

Pulsinelli, W.A., Brierley, J.B., and Plum, F. 1982. Temporal profile of neuronal damage in a model of transient forebrain ischemia. *Annals of Neurology*. 11: 491-498.

Roberts, J.E., Kukielczak, B.M., Chignell, C.F., Sik, B.H., Hu, D.N., and Principato, M.A. 2006. Simulated microgravity induced damage in human retinal pigment epithelial cells. *Molecular Vision*. 12: 633-638.

Sannita, W.G., Narici, L., and Picozza, P. 2006. Positive visual phenomena in space: A scientific case and a safety issue in space travel. *Vision Research*. 46: 2159-2165.

Smith, D.H., Chen, X.H., Nonaka, M., Trojanowski, J.Q., Lee, V.M., Saatman, K.E., Leoni, M.J., Xu, B.N., Wolf, J.A., and Meaney, D.F. 1999. Accumulation of amyloid beta and tau and the formation of neurofilament inclusions following diffuse brain injury in the pig. *Journal of Neuropathology & Experimental Neurology*. 58: 982-992.

Song, D., Song, Y., Hadziahmetovic, M., Zhong, Y., and Dunaief, J.L. 2012. Systemic administration of the iron chelator deferiprone protects against light-induced photoreceptor degeneration in the mouse retina. *Free Radical Biology and Medicine*. 53: 64-71.

Sparrow, J.R., Nakanishi, K., and Parish, C.A. 2000. The lipofuscin fluorophore A2E mediates blue light-induced damage to retinal pigmented epithelial cells. *Investigative*

Ophthalmology & Visual Science. 41: 1981-1989.

Stein, T.P. 2002. Space flight and oxidative stress. *Nutrition*. 18: 867-871.

Sundaresan, A. and Pellis, N.R. 2009. Cellular and genetic adaptation in low-gravity environments. *Annals of the New York Academy of Sciences*. 1161: 135-146.

Tanito, M., Nishiyama, A., Tanaka, T., Masutani, H., Nakamura, H., Yodoi, J., and Ohira, A. 2002. Change of redox status and modulation by thiol replenishment in retinal photooxidative damage. *Investigative Ophthalmology & Visual Science*. 43: 2392-2400.

Tanito, M., Takanashi, T., Kaidzu, S., Yoshida, Y., and Ohira, A. 2003. Cytoprotective effects of rebamipide and carteolol hydrochloride against ultraviolet B-induced corneal damage in mice. *Investigative Ophthalmology & Visual Science*. 44: 2980-2985.

Tombran-Tink, J. and Barnstable, C.J. 2006. Space flight environment induces degeneration in the retina of rat neonates. *Advances in Experimental Medicine and Biology*. 572: 417-424.

Ueta, T., Inoue, T., Furukawa, T., Tamaki, Y., Nakagawa, Y., Imai, H., and Yanagi, Y. 2012. Glutathione peroxidase 4 is required for maturation of photoreceptor cells. *Journal of Biological Chemistry*. 287: 7675-7682.

van Wijngaarden, P., Brereton, H.M., Coster, D.J., and Williams, K.A. 2007. Stability of housekeeping gene expression in the rat retina during exposure to cyclic hyperoxia. *Molecular Vision*. 13: 1508-1515.

Vandesompele, J., De Preter, K., Pattyn, F., Poppe, B., Van Roy, N., De Paepe, A., and Speleman, F. 2002. Accurate normalization of real-time quantitative RT-PCR data by geometric averaging of multiple internal control genes. *Genome Biology*. 3(7): RESEARCH0034.

Wang, A.L., Lukas, T.J., Yuan, M., Du, N., Tso, M.O., and Neufeld, A.H. 2009. Autophagy and exosomes in the aged retinal pigment epithelium: possible relevance to drusen formation and age-related macular degeneration. *PLoS ONE*. 4: E4160.

Wei, Y., Gong, J., Yoshida, T., Eberhart, C.G., Xu, Z., Kombairaju, P., Sporn, M.B., Handa, J.T., and Duh, E.J. 2011. Nrf2 has a protective role against neuronal and capillary degeneration in retinal ischemia-reperfusion injury. *Free Radical Biology and Medicine*. 51: 216-224.

Wiegand, R.D., Giusto, N.M., Rapp, L.M., and Anderson, R.E. 1983. Evidence for rod outer segment lipid peroxidation following constant illumination of the rat retina. *Investigative Ophthalmology & Visual Science*. 24: 1433-1435.

Wilkerson, M.K., Colleran, P.N., and Delp, M.D. 2002. Acute and chronic head-down tail suspension diminishes cerebral perfusion in rats. *American Journal of Physiology - Heart and Circulatory Physiology*. 282: 328-334.

Wise, K.C., Manna, S.K., Yamauchi, K., Ramesh, V., Wilson, B.L., Thomas, R.L., Sarkar, S., Kulkarni, A.D., Pellis, N.R., and Ramesh, G.T. 2005. Activation of nuclear transcription factor-kappaB in mouse brain induced by a simulated microgravity environment. *In Vitro Cellular & Developmental Biology - Animal*. 41: 118-123.

Yang, D., Elner, S.G., Chen, X., Field, M.G., Petty, H.R., and Elner, V.M. 2011. MCP-1-activated monocytes induce apoptosis in human retinal pigment epithelium. *Investigative Ophthalmology & Visual Science.* 52: 6026-6034.

Zhu, Y., Zhang, Y., Ojwang, B.A., Brantley, M.A., and Gidday, J.M. 2007. Long-term tolerance to retinal ischemia by repetitive hypoxic preconditioning: role of HIF-1alpha and heme oxygenase-1. *Investigative Ophthalmology & Visual Science.* 48: 1735-1743.